DEPLOYMENT AND DESIGN OF MULTIANTENNA SOLUTIONS FOR FIXED WIMAX SYSTEMS

M. Nicoli[1]**, L. Sampietro**[2]**, C. Santacesaria**[2]**, U. Spagnolini**[1]**, D. Archetti**[1]**, A. Bonfanti**[1]**, M. Sala**[1]

[1] *Dip. di Elettronica e Informazione, Politecnico di Milano, Milano, Italy*
[2] *Siemens Networks S.p.A., Cassina de' Pecchi (Milano), Italy*

Abstract: WiMax has already attracted the attention of operators and manifacturing industries for its promise of large throughput and coverage in broadband wireless access. However, towards the goal of an efficient deployment of this technology, a thorough analysis of its performance in presence of frequency reuse under realistic traffic conditions is mandatory. In particular, an important performance limiting factor is the inter-cell interference, which has strong non-stationary features. This paper investigates the deployment of multi-antenna base stations and the related design of signal processing algorithms for interference mitigation, for the uplink of IEEE 802.16-2004 systems. Extensive numerical results for realistic interference models show the advantages of the proposed multi-antenna system.

Keywords: communication systems, signal processing algorithms, adaptive arrays, interference, optimal filtering, equalization

I. INTRODUCTION

WiMax (Worldwide Interoperability for Microwave Access) is a standard-based technology that provides last mile broadband wireless access. In particular, the first version of the standard, IEEE 802.16-2004 [1] [2], was designed to provide broadband access to fixed subscriber stations (SS), by exploiting Orthogonal Frequency Division Multiplexing (OFDM), adaptive modulation and coding, and multiple antenna. Single WiMax links based on IEEE 802.16-2004 are by now well studied [3], but the impact of a deployment of multiantenna WiMax systems over a given geographical area is still under investigation. WiMax access points distributed over the coverage area form a cellular structure with a given frequency reuse factor (see Fig. 1). In such a scenario, the main technological challenge is the mitigation of multipath fading and out-of-cell interference. This issue is made even more challenging by the non-stationarity nature of interference, due to the asynchronous access of users in the interfering cells. In fact, in a typical scenario, out-of-cell SSs are expected to start and end their transmission on a time scale that cannot be controlled by the interfered cells.

In this paper we focus on the deployment and design of IEEE 802.16-2004 systems in presence of multiple antenna at the base station (BS), as this technology is known to reduce inter-cell interference and fading effects, by providing either beamforming or diversity gains. Diversity-oriented schemes use large antenna spacing to get fading uncorrelation and mitigate the impairments caused by channel fluctuations. On the other hand, when a small spacing is adopted, the fading is highly correlated and beamforming techniques can be employed for interference rejection. In this paper we show that the optimal antenna array deployment can be obtained as a trade-off
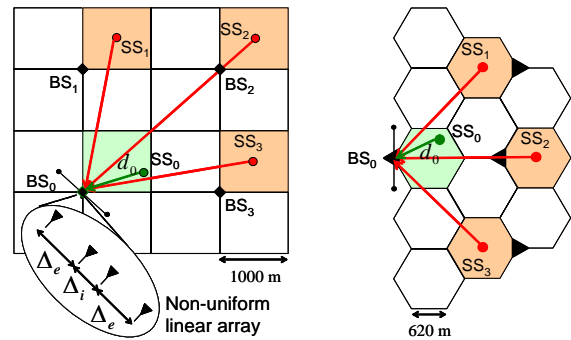

Fig. 1. Examples of uplink cellular layout with either square (left) or hexagonal (right) cells. Shaded cells represent the first ring of interference for reception of the user SS_0 by the base station BS_0. The base station BS_0 is equipped with a non-uniform linear array with $M = 4$ antennas and inter-element spacings Δ_e and Δ_i.

between diversity and interference rejection capability of the antenna array. Then we evaluate the average throughput for the overall cell obtained by the optimized array and the corresponding gain with respect to conventional (non-optimized) array receivers. Finally, signal processing techniques are investigated at the BS to efficiently cope with non-stationary interference.

II. SYSTEM AND SIGNAL MODEL

We consider the uplink of a fixed WiMax system conforming to the IEEE 802.16-2004 standard [1] [2]. Fig. 1 exemplifies the scenario of interest for: a square layout with cell side $r = 1$km and frequency reuse factor $F = 4$ (left); an hexagonal layout with cell side $r = 620$m and frequency reuse factor $F = 3$ (right). In this example, the

transmission by the subscriber station SS_0 to its own base station BS_0 is impaired by the interference from $N_I = 3$ out-of-cell subscriber stations $\{SS_i\}_{i=1}^{N_I}$. The base station BS_0 is equipped with a linear symmetric array of M antennas (covering either a 90 or a 120 degree sector in the examples of Fig. 1), while SSs have a single antenna.

Within a given OFDM symbol, the $M \times 1$ baseband signal received by the antenna array on the kth subcarrier $(k = 1, \ldots, K)$, on a given OFDM symbol, can be written as $\mathbf{y}_k = \mathbf{h}_k x_k + \mathbf{n}_k$, where $\mathbf{h}_k$ is a vector gathering the M (complex) channel gains between the transmitter SS_0 and the M antennas at BS_0, while x_k denotes the symbol transmitted by the desired station SS_0. The transmitted symbol x_k is chosen from the constellation of one of the modulation-coding scheme$\{T_i\}_{i=1}^7$ listed in Table I, based on the channel state, so as to satisfy a fixed bit error rate (BER$= 10^{-6}$). The noise vector $\mathbf{n}_k$ is assumed to be zero-mean Gaussian, temporally uncorrelated but spatially correlated with spatial covariance matrix $\mathbf{Q} = \mathrm{E}[\mathbf{n}_k \mathbf{n}_k^H]$. The other main system parameters are listed in Table II.

The multipath channel vector $\mathbf{h}_k$ is modelled as the superposition of N_p path contributions, each characterized by a direction of arrival (DOA) (θ_r), a delay (τ_r) and a complex fading amplitude (α_r):

$$\mathbf{h}_k = \sqrt{P^{(\mathrm{R})}} G_k \sum_{r=1}^{N_{\mathrm{p}}} \alpha_r \mathbf{a}(\theta_r) \exp\left(-j2\pi \frac{n_k}{N} \frac{\tau_r}{T}\right), \quad (1)$$

with $n_k \in \{-\frac{N}{2}, \ldots, \frac{N}{2} - 1\}$ denoting the frequency index for the kth useful subcarrier and N the total number of subcarriers. Here, $P^{(\mathrm{R})}$ denotes the average received power, G_k is the kth sample of the discrete Fourier transform of the waveform $g(\tau)$, that is the convolution of the transmitter and receiver filter impulse responses, sampled at the symbol frequency $\frac{1}{T}$. The $M \times 1$ vector $\mathbf{a}(\theta_r) = [a_1(\theta_r) \cdots a_M(\theta_r)]^T$ represents the array response to the direction of arrival θ_r for the symmetric linear array employed by BS_0. Being Δ_ℓ the spacing between the ℓth and the $(\ell+1)$th antennas, the gain $a_m(\theta_r)$,

for $m = 2, \ldots, M$, is given by

$$a_m(\theta_r) = \exp\left(j2\pi \frac{\sin(\theta_r)}{\lambda} \sum_{\ell=1}^{m-1} \Delta_\ell\right) \quad (2)$$

while for $m = 1$ it is $[\mathbf{a}(\theta_r)]_0 = 1$. In our performance analysis, amplitudes and delays $\{\tau_r, \alpha_r\}_{r=1}^{N_{\mathrm{P}}}$ are modelled according to the Stanford University Interim (SUI) channel model [4], while DOAs $\{\vartheta_\ell\}_{\ell=1}^{N_{\mathrm{P}}}$ are considered as uncorrelated Gaussian random variables distributed around the main direction SS_0-BS_0 with moderate angular spread σ_ϑ. The baseline case of signal coming from a single direction (i.e., with a null angular spread, $\sigma_\vartheta = 0$deg) will also be considered and referred to as a no-spatial-diversity (No-SD) channel. As further performance references, we consider two simplified Rayleigh-fading models that deviate from the SUI one and can be seen as extreme cases of frequency selectivity:

- No frequency diversity (No-FD): the channel gains are constant over the subcarriers (as for a null delay spread, i.e. $\tau_r = 0$, $\forall r$, or, equivalently, for a frequency-flat channel);
- Maximum frequency diversity (Max-FD): the channel gains are independent identically distributed over the subcarriers (as for the ideal case of a maximum delay spread).

The power $P^{(\mathrm{R})}$ received by BS_0 from SS_0 is

$$P^{(\mathrm{R})}[\mathrm{dBm}] = P^{(\mathrm{T})}[\mathrm{dBm}] + G - L(d_0) + S_0, \quad (3)$$

where $P^{(\mathrm{T})}$ denotes the transmitted power, $G = G^{(\mathrm{T})} + G^{(\mathrm{R})}$ the transmitter-receiver antenna gains, $L(d_0)$ the power loss over the distance d_0 between SS_0 and BS_0, $S_0 \sim \mathcal{N}(0, \sigma_s^2)$ the random fluctuations due to shadowing. As recommended in [1], the path-loss is modelled

TABLE II
RELEVANT SYSTEM PARAMETERS.

Carrier frequency f_c	3.5GHz
Sampling frequency $1/T$	4MHz
N. of subcarriers N	256
N. of useful subcarriers K	192 data +8 pilots
N. of guard-band subcarriers	28+27
Subcarrier spacing	15.625kHz
Useful OFDM symbol time	$64\mu s$
Cyclic-prefix time	$8\mu s$
SS omnidir. antenna gain $G^{(T)}$	2dBi
BS directional antenna gain $G^{(R)}$	16dBi
Path loss exponent γ	4
Noise figure	7dB
Shadowing std deviation σ_s	8dB
SS maximum power $P_T^{(\mathrm{max})}$	27dBm

TABLE I
TRANSMISSION MODES.

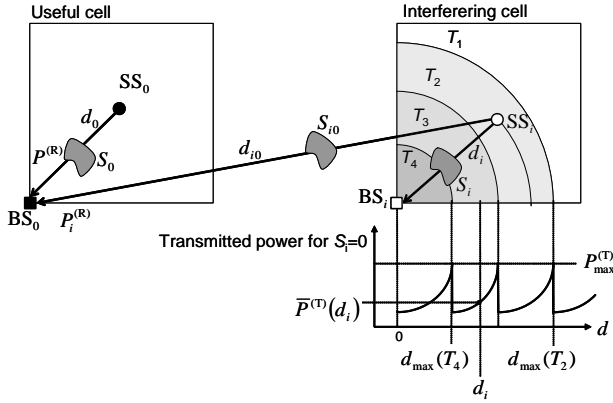| TX mode	Mod scheme	RS-CC coding rate	Through-put [Mbit/s]	SNR[dB] @BER=10^{-6} (Max-FD)
T1	BPSK	1/2	1.2	5.6
T2	QPSK	1/2	2.6	11.2
T3	QPSK	3/4	3.9	18.5
T4	16QAM	1/2	5.2	17.0
T5	16QAM	3/4	7.9	25.2
T6	64QAM	2/3	10.6	25.8
T7	64QAM	3/4	11.9	30.5

Fig. 2.   Shadowing effects on the user SS_0 and the interferer SS_i channels, for a square cellular layout.

according to the Hata-Okamura model [5]

$$L(d) = 20 \log_{10} \frac{4\pi d_{\text{ref}}}{\lambda} + 10\gamma \log_{10} \frac{d}{d_{\text{ref}}} + 6 \log_{10} \frac{f_c}{2} \tag{4}$$

with λ denoting the wavelength, γ the path-loss exponent, d_{ref} a reference distance, and f_c the carrier frequency [GHz]. Notice also that $P^{(\text{T})}$ is limited by the maximum power available at the SS's, i.e. $P^{(\text{T})} \le P_{\text{max}}^{(\text{T})}$. Thus, power control for the compensation of the path-loss $L(d_0)$ and the shadowing S_0 in (3) is possible only within this maximum power constraint.

The focus of this paper is on the effect of the noise $\mathbf{n}_k$. This is given by the sum of the background noise and the inter-cell interference generated by users $\{SS_i\}_{i=1}^{N_I}$, that are active in the nearby cells on the same bandwidth and the same time-slot as the desired transmission. Thereby, the noise covariance is $\mathbf{Q} = \sigma_n^2 \mathbf{I}_M + \mathbf{Q}_I$, where σ_n^2 is the variance of the background noise while $\mathbf{Q}_I$ denotes the contribution from the N_I active out-of-cell interferers. Propagation from each interferer to BS_0 is modelled similarly to the user SS_0, in terms of DOAs and average powers. DOAs are again assumed to be Gaussian distributed around the main direction SS_i-BS_0. The main difference with respect to the user SS_0 channel is given by the interferer shadowing fluctuactions which cannot be controlled by the base station BS_0. More specifically, the power received from the ith interferer depends on the transmitted power $P_i^{(\text{T})}$, the power loss over the distance d_{i0} (see Fig. 2) and the shadowing $S_{i0} \sim \mathcal{N}(0, \sigma_s^2)$ over the link SS_i-BS_0:

$$P_i^{(\text{R})}[\text{dBm}] = P_i^{(\text{T})}[\text{dBm}] + G - L(d_{i0}) + S_{i0}. \tag{5}$$

In order to satisfy the BER constraint at the base station BS_i, the power $P_i^{(\text{T})}$ transmitted by SS_i is chosen so as to compensate (up to the maximum available power $P_{\text{max}}^{(\text{T})}$) the path loss and the shadowing S_i over the distance d_i. As a consequence, the shadowing effects on the interferer power $P_i^{(\text{R})}$ are higher than those on the useful signal

power $P^{(\text{R})}$, as they are the superposition of the two fluctuations S_i and S_{i0} (see Fig. 2).

III. ANTENNA ARRAY DESIGN

In this section, we consider the selection of the optimal antenna deployment at the base station BS_0 for the square layouts in Fig. 3, with reuse factor $F = 1$ (top) and $F = 4$ (bottom), and for the hexagonal layouts in Fig. 4, with reuse factor $F = 1$ (top) and $F = 3$ (bottom). BS_0 is assumed to be equipped with a symmetric linear array of $M = 4$ elements, with internal spacing Δ_i and external spacing Δ_e, as the one shown in Fig. 1. The desired user SS_0 is uniformly distributed within the cell, while the interferers $\{SS_i\}_{i=1}^3$ are fixed at the centre of their cells. The channel model, for both user and interferers, is characterized by null angular spread (No-SD), and fading uncorrelation over the subcarriers (Max-FD). Shadowing is not accounted for ($\sigma_s = 0$), all terminals are assumed to transmit at maximum power $P_{\text{max}}^{(\text{T})}$. Exemplifying drawings on the right of each plot will be used in the figures all over the paper to recall the space/frequency characteristics of the simulated propagation environment.

To reduce the interference effects, BS_0 applies a spatial filter to the received signal. The optimal beamforming technique is the minimum variance distortionless (MVDR) filter, $\hat{x}_k = \left(\mathbf{h}_k^{\text{H}} \mathbf{Q}^{-1} \mathbf{h}_k\right)^{-1} \mathbf{h}_k^{\text{H}} \mathbf{Q}^{-1} \mathbf{y}_k$, which minimizes the output power subject to the constraint of unitary gain in the steering direction SS_0-BS_0 [6]. This leads to effective interference-rejection capabilities, as nulls are steered in directions of strong interferers. The interference-rejection capability may be quantified in terms of signal-to-interference-plus-noise ratio (SINR) at the output of the spatial filter: $\rho_k = \mathbf{h}_k^{\text{H}} \mathbf{Q}^{-1} \mathbf{h}_k$. This depends on the channel response ($\mathbf{h}_k$), the spatial pattern of the interference ($\mathbf{Q}$) and the antenna spacing. The first two quantities are determined by the cellular layout geometry, the SS position and the propagation environment, while the antenna spacings are free parameters that can be designed for a specific layout/environment so as to maximize the SINR performance.

The array optimization can be carried out by evaluating the SINR ρ_k, averaged with respect to the fading and the SS_0 position, for each spacing pair (Δ_e, Δ_i). The resulting SINR values for the square and hexagonal layouts herein considered are shown in gray scale in Figs. 3-4; it can be seen that the minimum-length array that maximizes the average SINR is a uniform linear array (ULA) having $\Delta_i = \Delta_e = \Delta_{\text{opt}}$ with optimal spacing Δ_{opt} that depends on the specific layout: $\Delta_{\text{opt}} = 2.2\lambda$ (top) and $\Delta_{\text{opt}} = 1.8\lambda$ (bottom) for the square layouts in Fig. 3 (λ is the carrier wavelength); $\Delta_{\text{opt}} = 1.9\lambda$ (top) and $\Delta_{\text{opt}} = 1.4\lambda$ (bottom), for the hexagonal layouts in Fig. 4. This confirms the analytical results of [7], where the optimal spacing is found to be $\Delta_{\text{opt}} = n\lambda / \sin(\Delta\theta)$
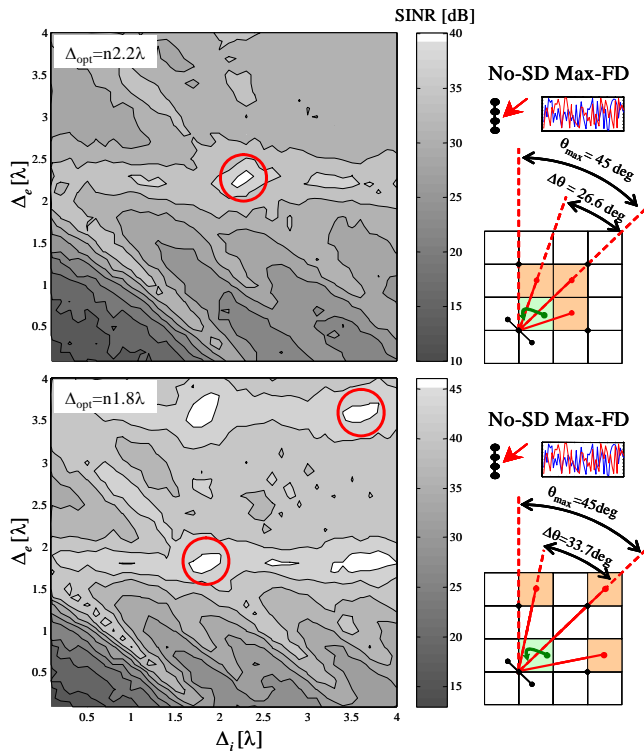
Fig. 3. Average SINR at the output of the MVDR filter versus the antenna spacings Δ_e and Δ_i ($M = 4$), for a square layout with reuse factor $F = 1$ (top) or $F = 4$ (bottom).

Fig. 4. Average SINR at the output of the MVDR filter versus the antenna spacings Δ_e and Δ_i ($M = 4$), for an hexagonal layout with reuse factor $F = 1$ (top) or $F = 3$ (bottom).

where n is a non-zero integer and $\Delta\theta$ the angular separation between interferers calculated as indicated in the drawings on the right of Figs. 3-4.

To better explain the optimization result, let us consider the layouts having $N_I = 3$ interferers in Figs. 3-4. The spacing Δ_{opt} turns out to be the best one as it introduces a certain degree of angular equivocation in the directivity function of the array such that the three interferers with DOAs $[\theta_1, \theta_2, \theta_3] = [-\Delta\theta, 0, +\Delta\theta]$ are grouped together along the unique direction $\theta = 0$. The spatial wave numbers associated to the DOAs of the interferers SS_1 and SS_3 are indeed $\omega_1 = \omega_3 = 2\pi \frac{\Delta_{opt}}{\lambda} \sin\theta_i = \pm 2\pi n$ and coincide with that of the broadside interferer SS_2 ($\omega_2 = 0$). This effect makes interference mitigation more effective, as one null of the directivity function on the broadside is enough to virtually reject three interferers, thus leaving other degrees of freedom to increase the spatial diversity.

It can be observed that the optimal antenna array is wider with respect to a standard antenna deployment used for beamforming purposes. The conventional spacing for beamforming is indeed the one that maximizes the DOA resolution under the non-alias constraint, i.e., $\Delta_{max} = \lambda/[2\sin(\theta_{max})]$ where θ_{max} is the largest DOA admissible for the considered cellular layout. In particular, it is $\Delta_{max} = \lambda/2$ when the antenna array covers the whole
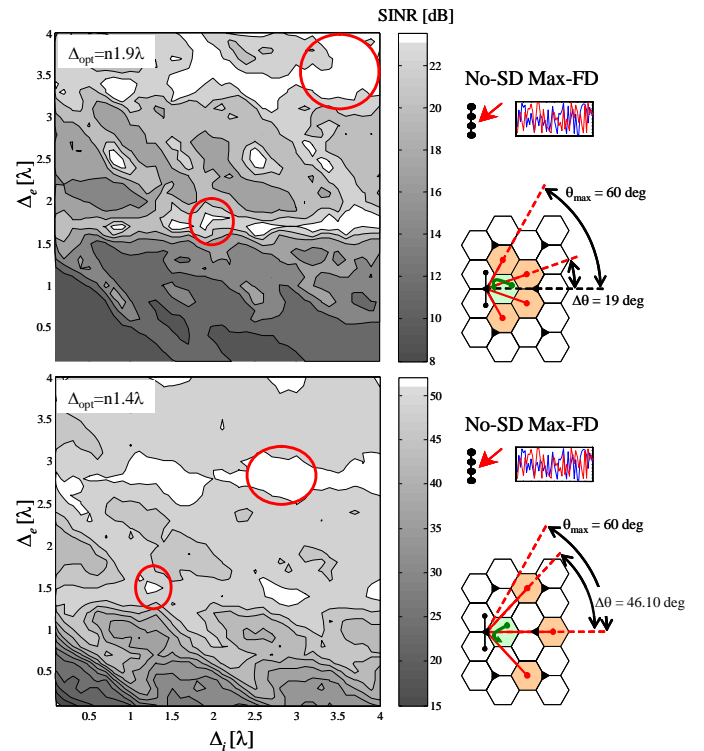
sector of 180deg ($\theta_{max} = 90$deg), while for the plannings in Figs. 3 and 4 it is: $\Delta_{max} = 0.71\lambda$ for the square layout ($\theta_{max} = 45$deg) and $\Delta_{max} = 0.58\lambda$ for the hexagonal layout ($\theta_{max} = 60$deg). The numerical results in Figs. 3-4 show that the conventional spacing Δ_{max} provides lower SINR performance with respect to the optimized deployment using Δ_{opt}.

IV. COVERAGE ANALYSIS

Let us now compare the average cell throughput provided by the optimized ULA with inter-element spacing Δ_{opt} with that obtained by a conventional ULA with spacing Δ_{max}. We consider the square and hexagonal layouts represented at the bottom of Figs. 3 and 4, under the same assumptions made in the previous section, i.e.: interferers placed at the center of their respective cells, channel model No-SD Max-FD without shadowing, maximum power transmission.

For each position of SS_0, we evaluate the average SINR at the output of the MVDR filter. Then, using pre-evaluated BER vs. SINR average performance, the best transmission mode among those listed in Table I is selected as the one satisfying the constraint BER$\leq 10^{-6}$ and providing the highest bit-rate. This allows to obtain, for all the positions of the user in the cell and all the transmission modes, the coverage maps shown in Fig. 5 (for the
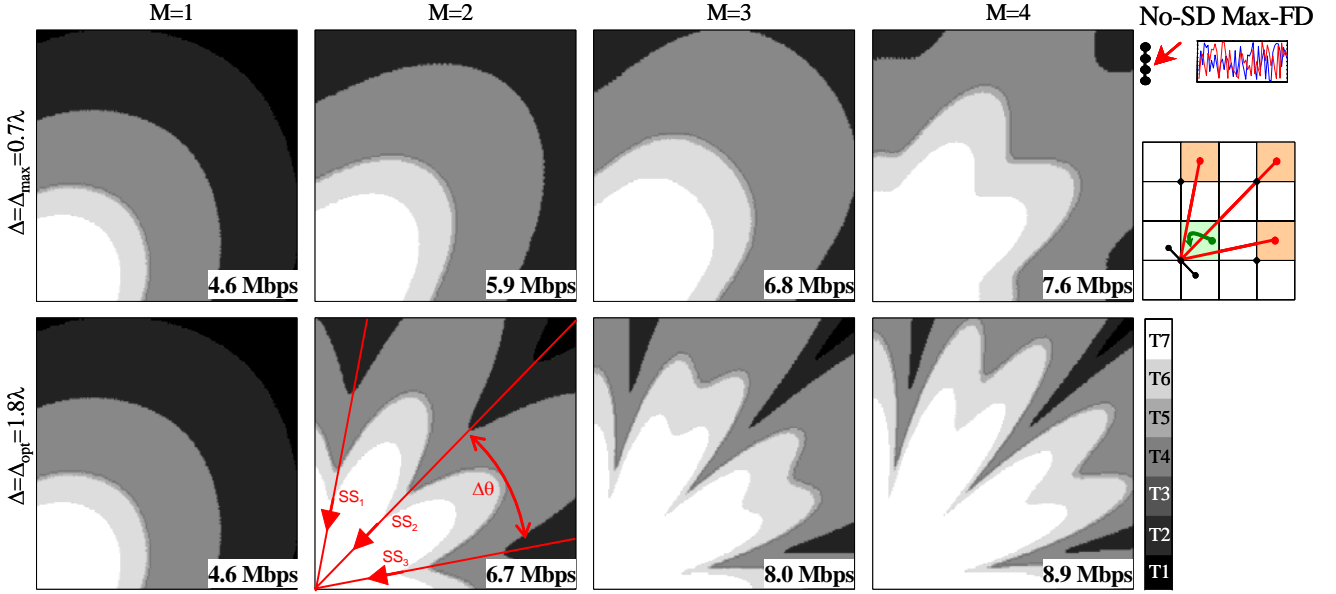
Fig. 5. Coverage for all transmission modes $\{T_i\}_{i=1}^7$ represented in gray-scale for the square layout with reuse factor $F = 4$. The arrows indicate the directions of arrival of the interferers. The BS_0 antenna array has a number of elements ranging from $M = 1$ (left) to $M = 4$ (right), and inter-element spacing optimized for beamforming purposes (top) or optimized for coverage (right).

square layout with $F = 4$) and Fig. 6 (for the hexagonal layout with $F = 3$). The array at BS_0 has a number of antennas ranging from $M = 1$ (left) to $M = 4$ (right), with inter-element spacing equal to Δ_{max} (top) or Δ_{opt} (bottom). The average throughput [Mbit/s] for the overall cell, indicated on the bottom of each map, is obtained as a weighted average of the throughputs associated to the different transmission modes, using as weighting factors the normalized areas where the modes are supported.

As expected, the optimized array is shown to provide substantial throughput improvements with respect to the conventional beamforming-oriented array. Furthermore, looking at the coverage maps for $M = 2$, it can be easily seen that, even using only two elements, the optimized array is able to considerably reduce the interference from all the three out-of-cell users by exploiting the spatial aliasing induced by large antenna spacing: the coverage map is indeed periodic in angles with period equal to the interferers' angular separation ($\Delta\theta = 33.7$deg for the square layout and $\Delta\theta = 60$deg for the hexagonal layout), so that a single null can be put simultaneously over the three directions of the interferers. This is not possible with a conventional array, where the period is $2\theta_{max}$ (90deg for the square layout and $\Delta\theta = 120$deg for the hexagonal layout), and a single degree of freedom is not enough to reject all the interferers. The interference rejection capability increases with the number M of antennas so as to lead asymptotically to the interference-free case (i.e., in presence of background noise only). Notice also that, as observed from the coverage maps along the interferer directions, the performance improvement is clearly

not possible when the user SS_0 is aligned with one of the interferers. Along the interfering DOAs the throughput is approximately the same obtained for $M = 1$, regardless of the number of antennas, while out of the interfering beams the performance improvement provided by the optimized array is remarkable.

V. COVERAGE ANALYSIS IN SHADOWING SCENARIO

We now consider the impact of the SINR fluctuations due to shadowing effects on the system performance. The analysis is here referred to the square planning with reuse factor $F = 4$, with fixed interferers positions. The channel model is SUI-3, with angular spread $\sigma_\vartheta = 5 \deg$ and shadowing standard deviation $\sigma_s = 8$dB; shadowing effects over the link SS_0-BS_0 are assumed to be perfectly compensated by power control (i.e., the shadowing is simulated for interferers only). The receiver consists of MVDR filtering, soft demodulation and convolutional/Reed-Solomon (CC/RS) decoding.

Fig. 7 shows the outage probability versus the user position within its cell for an optimized ULA with $M = 4$ (top) and for the single antenna case (bottom). The outage probability is here defined as the probability $P_{out} = \mathrm{pr}(P_b > \bar{P})$ that the BER P_b (after channel decoding) exceeds the threshold $\bar{P} = 10^{-4}$. The analysis in terms of outage probability yields similar conclusions to the investigation of throughput coverage, lending evidence to the performance benefits of a multiantenna receiver with optimized spacings.
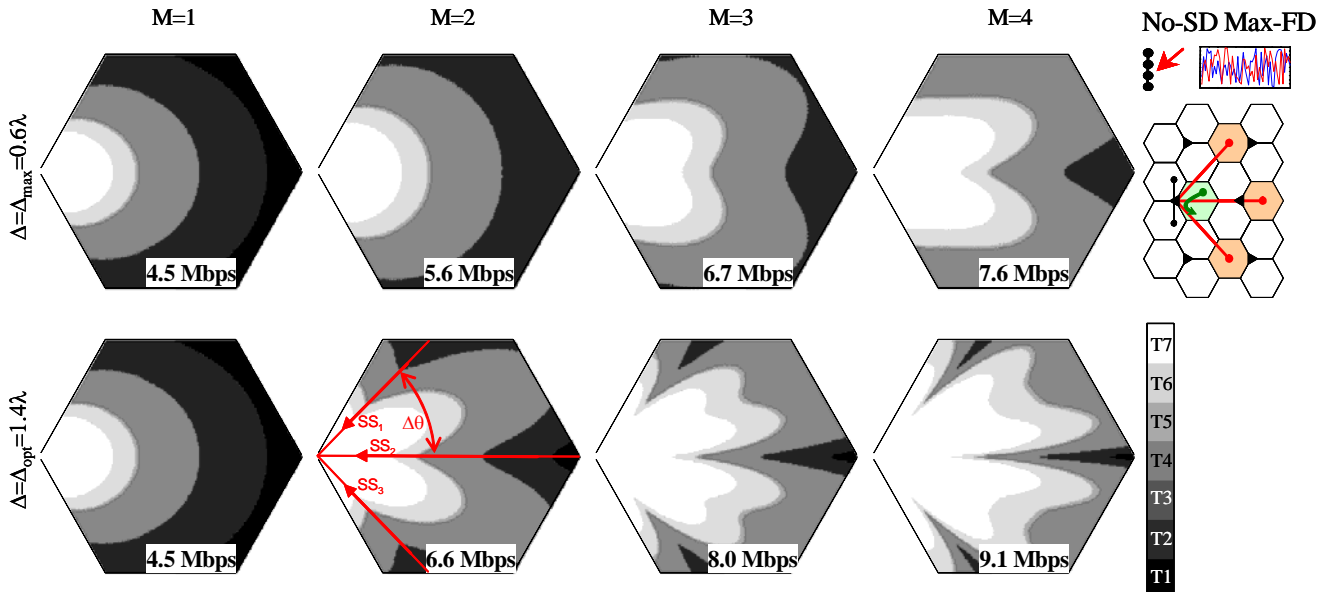
Fig. 6. Coverage for all transmission modes $\{T_i\}_{i=1}^7$ represented in gray-scale for the hexagonal layout with reuse factor $F = 3$. The arrows indicate the directions of arrival of the interferers. The BS_0 antenna array has a number of elements ranging from $M = 1$ (left) to $M = 4$ (right), and inter-element spacing optimized for beamforming purposes (top) or optimized for coverage (right).

VI. NON-STATIONARY INTERFERENCE MITIGATION

The channel gains $\mathbf{h}_k$ and the interference covariance matrix $\mathbf{Q}$, needed for spatial filtering implementation, may be estimated from pilot subcarriers through least-squares (LS) methods. In IEEE 802.16-2004 systems, the transmitted frame is organized in bursts, each containing a long preamble followed by a sequence of OFDM data symbols. Eight pilot subcarriers are also embedded in each data symbol (see Table II).

In the fixed access scenario targeted in this paper the channel coherence time is large enough to make the channel invariant over the whole frame interval. The vector $\mathbf{h}_k$ can thus be evaluated by performing a separate LS estimate from each preamble and then averaging the estimates over the preambles. However, the statistical features of the interference, and in particular the covariance matrix $\mathbf{Q}$, can vary within the frame due to the asynchronous access of users in neighboring cells: at any time instant (here assumed to be an integer multiple of the OFDM time symbol), a SS from an interfering cell might end its transmission and be replaced by another SS transmission, thus generating abrupt changes in the signal interfering on the user SS_0.

To cope efficiently with this non-stationary interference, we employ the estimation method proposed in [8] which allows to track the power/spatial features of the interferers by exploiting both the preambles and the pilots embedded in each burst. At first, the signals measured in all the preambles in the frame are used to obtain an estimate of the channel $\mathbf{h}_k$ (by averaging over the preambles) and

a first estimate of the interference covariance matrix $\mathbf{Q}$ in each preamble. The matrix $\mathbf{Q}$ is then updated within each OFDM symbol, by using the embedded pilots. Abrupt variations of the interference are detected by comparing the covariance estimate obtained from the pilots of the current OFDM symbol with the one extracted from the previous OFDM symbol, in order to decide whether the spatial structure of the interference has changed or not: if the correlation ρ between the two subsequent covariance estimates is larger than a given threshold $\bar{\rho}$, the interference covariance estimate is refined by averaging, otherwise is re-initialized according to the new estimate value.

The performance of this estimation/tracking approach is here evaluated for the square cellular layout with $F = 4$. The optimized ULA with $M = 4$ and $\Delta_{\text{opt}} = 1.8\lambda$ is adopted by BS_0. The user SS_0 transmits at maximum power $P_{\max}^{(\mathrm{T})}$ using the transmission mode T_2. Interferers $\{SS_i\}_{i \in I_t}$ are uniformly distributed in their cells; their power (subject to log-normal shadowing with $\sigma_s = 8$dB) and transmission mode are adaptively selected based on the channel state so as to guarantee a BER$\leq 10^{-3}$. Multipath channels are modelled according to the SUI-3 model with angular spread $\sigma_\vartheta = 5 \deg$ for both user and interferers. The user SS_0 is placed in broadside at a distance $d = 0.8$ km from BS_0. The simulated frame is composed $L = 10$ bursts of 10 symbols. In each of the interfering cell, the active user SS_i can stop its transmission and be replaced by a new terminal with probability $p = 1/30$; it follows that the probability of change of any interferer power/DOA (i.e., the probability of change for $\mathbf{Q}$) is $3p = 0.1$. The correlation threshold for change
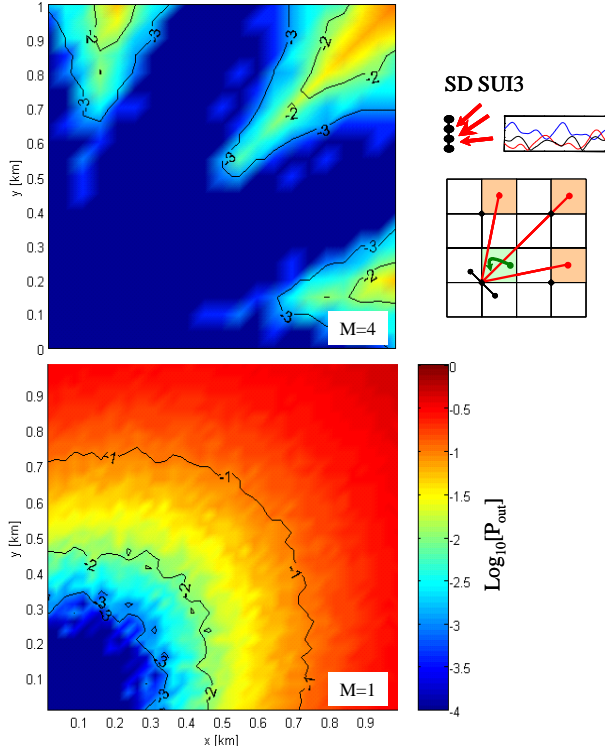
Fig. 7. Outage probability versus the user position for the square cell planning with reuse factor $F = 4$: optimized ULA with $M = 4$ (top); single-antenna receiver (bottom).

Fig. 8. Comparison of channel (top) and interference covariance (bottom) estimation techniques, in terms of average BER versus the user SS_0 angular position, for the square layout with reuse factor $F = 4$.

detection is set to $\bar{\rho} = 0.7$.

Fig. 8 compares the performance of channel/interference estimation with the ideal case of perfect channel state information in terms of average BER (after channel decoding) versus the angular position of SS_0. The top figure compares different channel estimation approaches: estimation from the current preamble only (dashed line); average over L preambles (thin line); known channel (thick line). In the bottom figure, the estimate of the interference matrix $\mathbf{Q}$ is obtained using three different approaches: estimation only from the preamble of the current burst (dotted line); re-estimation from the pilots within each OFDM symbol, without memory (dashed-dotted line); tracking over all OFDM symbol with interference-change detection (thin line). The BER results confirm that the joint use of the multi-preamble average for the channel estimate and the detection/tracking method for the interference estimate is an effective approach for time-varying interference mitigation.

VII. CONCLUSION

In this work, the antenna deployment and the receiver processing design of fixed WiMax systems with multiple antenna at the base station have been investigated for the IEEE 802.16-2004 standard. The inter-element spacing at th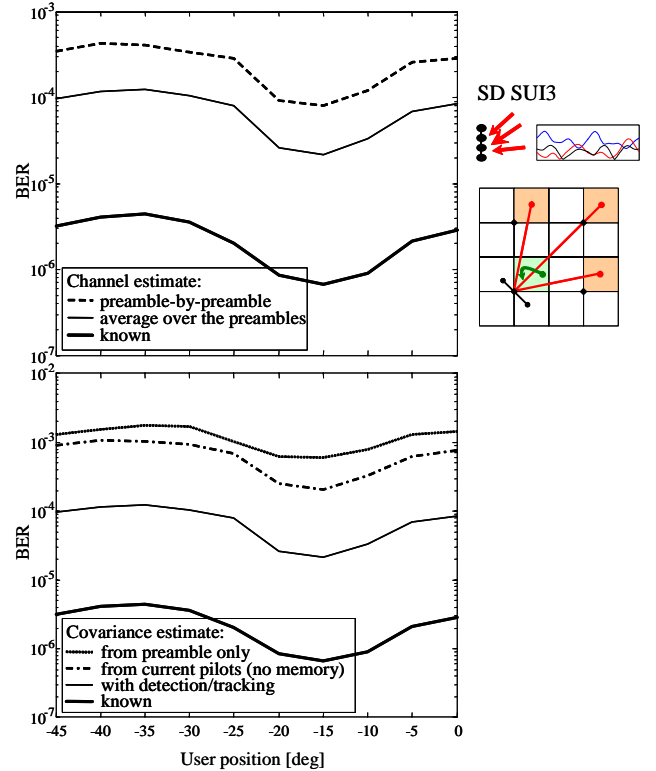e receiving antenna array has been derived so as to maximize the interference rejection capability. An adaptive array processing technique based on MVDR beamforming has also been analyzed to cope with asynchronous out-of-cell interference. Thorough simulation results for square and hexagonal cell layouts in different propagation environments have proved the advantages of the proposed antenna array scheme.

REFERENCES

[1] IEEE Std 802.16[TM]-2004, "802.16[TM] IEEE standard for local and metropolitan area networks Part 16: Air interface for fixed broadband wireless access systems," Oct. 2004.

[2] IEEE P802.16-2004/Cor1/D5 (Draft Corrigendum to IEEE Std 802.16-2004), "Corrigendum to IEEE standard for local and metropolitan area networks - Part 16: Air interface for fixed broadband wireless access systems," Sep. 2005.

[3] A. Ghosh, D.R Wolter, J. G. Andrews, R. Chen, "Broadband wireless access with WiMax/802.16: current performance benchmarks and future potential," *IEEE Communications Magazine*, Vol. 43, No. 2, pp. 129-136, Feb. 2005.

[4] IEEE 802.16.3c-01/53, IEEE 802.16 Broadband Wireless Access Working Group, "Simulating the SUI channel models," April 2004.

[5] A. Goldsmith, *Wireless communications*, Cambridge University Press, 2005.

[6] H. L. Van Trees, *Optimum array processing*, Wiley, 2002.

[7] S. Savazzi, O. Simeone, and U. Spagnolini, "Optimal design of linear arrays in a TDMA cellular system with Gaussian interference," *Proc. IEEE SPAWC*, pp. 485-489, June 2005.

[8] M. Nicoli, M. Sala, L. Sampietro, C. Santacesaria, O. Simeone, "Adaptive array processing for time-varying interference mitigation in IEEE 802.16," *Proc. IEEE Int'l. Symp. on Pers. Indoor and Mobile Radio Commun. (PIMRC'06)*, Helsinki, Sep. 2006.